P-Type Electrical Conduction in Transparent Conducting Oxides

Diedrich A. Schmidt

Dr. Janet Tate, Advisor

31 May 2000

Approved____________________ Date__________

Abstract

We implemented the method of van der Pauw testing to determine the resistivity and carrier type of transparent conducting oxides (TCO). This is a four-point probe technique used on flat, homogeneous, and isotropic materials. Two contacts are used to drive the sample with a given current, while the other two measure the voltage. By including the other two contact permutations, and repeating the measurements with opposite current flow, geometric variations can be averaged out. Calibration measurements on GaAs yielded a resistivity of $5.47 \times 10^{-2} \pm 4 \times 10^{-4}$ Ωcm and a Hall mobility of $4.36 \times 10^{3} \pm 49$ cm^2/Vs, and those on indium tin oxide (ITO, an n-type TCO) gave $1.061 \times 10^{-4} \pm 3 \times 10^{-8}$ Ωcm for resistivity and 33.3 ± 0.2 cm^2/Vs for mobility, all close to expected values for these materials. For the p-type TCO, $CuAlO_2$, resistivities ranged between 7.8 ± 0.1 Ωcm and 44.4 ± 0.4 Ωcm and Hall mobilities (expected to be ~1 cm^2/Vs) were inconclusive. Measurements on $(YCa)CuO_2$ and $(YCa)SnCuO_2$ yielded resistivities between 5.0 ± 0.9 Ωcm to 48.9 ± 2.2 Ωcm and $6.63 \times 10^{-4} \pm 4.3 \times 10^{-6}$ Ωcm to $9.1 \times 10^{-4} \pm 5.6 \times 10^{-5}$ Ωcm, respectively, but the Hall mobilities were inconclusive for both samples. Thermopower measurements yielded n-type conductivity for GaAs and ITO and p-type for $CuAlO_2$.

Transparent conducting oxides (TCO) are important and interesting materials. By definition, a TCO must be conductive and transparent. These two parameters are usually mutually exclusive, i.e. if a material is conductive it tends to be less transparent, and vice versa. Conductive materials such as metals have many electrons in their conduction band which easily re-radiate electromagnetic energy and therefore are not transparent. Conversely, insulating materials such as glass have no electrons in their conduction band, allowing light to "pass through" and not be re-radiated. The lack of electrons in the conduction band of insulators can be attributed to the large band gap between the valence and conduction bands. This band gap is large enough to prevent electrons from accessing the conduction band under standard temperature and pressure. The conductivity comes from an indirect band gap close the conduction band. Due to the character of an indirect band gap, the transition of an electron to the conduction band by optical stimulation is very unlikely, and thus the material is transparent and conducting at the same time. The unique character of TCOs allows them to be used in a wide variety of applications. These range from solar cell fabrication to windshield defrosters and electrodes in flat panel displays (Morgan & Brodie). The most common TCO manufactured today is indium tin oxide (ITO). ITO is n-type because the majority of charge carriers in the material are electrons. This material has very low resistivity ($\sim 1 \times 10^{-4}$ Ωcm) and mobility (24 cm^2/Vs), along with being quite transparent in the visible spectrum (over 85%). Compare these values with copper, which has a resistivity of 1.725×10^{-6} Ωcm and Hall mobility of 29.68 cm^2/Vs at room temperature.

The complementary materials to an n-type TCOs are p-type TCOs. The major difference is that p-type TCOs have holes as the majority of charge carriers rather than electrons. There

does not currently exist a p-type oxide material with resistivity and mobility values comparable to ITO. The desire for designing a matching p-type oxide is evident for use in creating a transparent transistor (Thomas, 1997). Due to the fact that optically transparent materials have a band gap $\geq$3.1 eV means that radiation only in the ultraviolet range will be absorbed by the material. Transparent diodes can thus be manufactured to emit or collect ultraviolet radiation (Kawazoe, et. al.; Kudo, et. al.).

There are currently a few different p-type TCOs being researched as matching partners for ITO. For example, some experimental materials are $YCaCuO_2$, $YCaSnCuO_2$, $CuAlO_2$, and $SrCu_2O_2$. They all have the delafossite structure. The basic composition of a delafossite is ABO_2, where A is a monovalent metal ion and B is a trivalent ion. As described by Benko and Koffyberg (Benko and Koffyberg, 1985):

> In the delafossite structure the B ions are octahedrally surrounded by oxygen ions, and the octahedra are connected to form layers of net composition $[BO_2]^-$. The monovalent ions also form layers (perpendicular to the crystallographic c-axis) in between the $[BO_2]^-$ sheets; each A ion forms a linear O-A-O arrangement with oxygen ions in neighboring layers.

The goal then is create a p-type oxide that has similar characteristics for resistivity and mobility as does ITO.

To confirm the proper conduction of the samples, the van der Pauw technique was used in measuring both the resistivity and Hall coefficient. In 1958, van der Pauw solved the potential problem for a thin layer of material of arbitrary shape (Look, 1989) (see Fig. 1). The benefits are

that most geometric variations can be canceled out and thickness is the only dimension required for calculations. The validity of this method requires the samples to be flat, singly connected (no holes), homogenous and isotropic, and have line electrodes on the periphery projecting to point contacts on the surface, or true point contacts on the surface (Look, 1989). The latter requirement is the most difficult to satisfy. For each of the samples under test, contacts of approximately 1 mm (l_c) diameter were placed on samples of 7 by 7 mm (l_s). The contacts were made with either conductive silver paint (Circuit Works Conductive Silver Pen or M.E. Taylor Engineering, Inc. conductive silver paint) or evaporated copper. Corrections to resistivity and Hall coefficient are determined from Figures 4a) and 4b). For our samples, $l_c/l_s \approx 0.14$, and from the graphs the decrease in resistivity and increase in Hall coefficient will be 1-2% and 10-12% respectively (Look, 1989). A small decrease in error can be realized by using a circular disc of diameter l_s with contacts of length l_c placed at the periphery, for which van der Pauw has calculated the corrections to be:

$$\frac{\Delta\rho}{\rho} \approx -\frac{1}{16 \ln 2}\frac{l_c^2}{l_s^2} \quad (per\ contact) \qquad \frac{\Delta R_H}{R_H} \approx \frac{2}{\pi^2}\frac{l_c}{l_s} \quad (per\ contact)$$

Thus for our samples ($l_c/l_s \approx 0.14$) and $\Delta\rho/\rho \approx -0.74\%$ and $\Delta R_H/R_H \approx 11.6\%$ (Look, 1989). The difference in numbers between the graph and the above equations is that the graphs are for square samples and the equations are for circular samples. The following discussion of the van der Pauw method for resistivity and Hall coefficient is adapted from Look.

Resistivity (ρ, Ωcm) measurements are made by applying a current through two adjacent

contacts and measuring the voltage through the other two (see Fig. 1a). The relationship between the current and voltage is found by first mapping the given (generally more complex) geometry onto a simpler geometry. The Laplace equation can then be solved for the simpler geometry. The results of van der Pauw's method are as follows: Let $R_{ij,kl} = V_{kl}/I_{ij}$, where current enters contact i and leaves j, and $V_{kl} = V_k - V_l$. When no magnetic field is present, the resistivity is calculated as follows

$$\rho = \frac{\pi d}{ln2}[\frac{R_{21,34} + R_{32,41}}{2}]f \qquad (1a)$$

where d is the thickness of the film and

$$R_{21,34} = \frac{V_{34}}{I_{21}} \qquad (1b)$$

where f is a geometrical factor ($f = 1$ for square samples, $f < 1$ for all other shapes). For accurate measurements, it is useful to average over the remaining two contact permutations and to reverse the current for all four permutations. The resistivity then becomes:

$$\rho = \frac{\pi d}{ln2}\frac{1}{8}[(R_{21,34} - R_{12,34} + R_{32,41} - R_{23,41})f_A + (R_{43,12} - R_{34,12} + R_{14,23} - R_{41,23})f_B] \qquad (2)$$

again, f_A and f_B are factors to account for geometric variations, but are set to unity in all of the calculations in this paper because of the symmetry of contact placement (in general $f_A \neq f_B$).

Equation (2) is needed to calculate the Hall mobility, μ_H, but the Hall coefficient is also needed. The Hall coefficient is calculated from measuring the Hall effect on a conductor. The Hall effect was first measured by E. H. Hall in 1879 while investigating the forces acting on a current carrying conductor in a magnetic field (Putley, 1960). If a conductor, carrying a current density **J** in the **y** direction is in a uniform, static magnetic field $\mathbf{B} = B_o\mathbf{x}$, there will be a force on the charge carriers inside the conductor. The Lorentz force acts on the charge carriers according to:

$$\mathbf{F} = q\mathbf{v} \times \mathbf{B}$$

where, q = charge in Coulombs and $\mathbf{J} = q\mathbf{v}$

The charge carriers experience a force in the **-z** direction. Both electrons and holes (whichever are present) are deflected in the same direction (see Fig. 2). Electrons are deflected in the same direction as holes because they have the opposite sign for charge ($-q$) and they flow in the opposite direction (**-v**) therefore resulting in the same direction for the force. Since there is no where for the deflected charges to go, there is a build-up of charge on the z = 0 and z = a surfaces of the material. Eventually, a potential difference will develop between the two surfaces which will counteract the Lorentz force from the magnetic field (Hurd, 1972) (see Fig. 2). This potential difference, perpendicular to both the magnetic field and current, is the measured Hall voltage used to calculate the Hall coefficient (Look, 1989). For the Hall bar geometry of Fig. 2, the voltage is measured on the surfaces which are perpendicular to both the applied magnetic field and the flow of current.

The van der Pauw method can also be used to calculate the Hall coefficient (R_H, cm^3/C) if

a slight change in configuration is made. To measure the Hall voltage, the current contacts and voltage contacts need to be crossed (see Fig. 1b). Following discussions in DeMey (1983) and Look (1989), leads to the following equation of the current density field **j** for isotropic semiconductors:

$$\mathbf{j} = \sigma\mathbf{E} - \sigma\mu_H(\mathbf{E} \times \mathbf{B})$$

We can rewrite this as:

$$\mathbf{E} = \rho\mathbf{j} + \rho\mu_H(\mathbf{j} \times \mathbf{B})$$

where **j** is the current density field and $\rho = 1/\sigma$

This equation is correct to first order in $\mu_H B$, and neglects magnetoresistive terms ($\mu_H^2 B^2$) (De Mey, 1983 & Look,1989). When no magnetic field is present, the voltage difference between contacts 2 and 4 is:

$$(V_4 - V_2)_{B=0} = \int_{r_2}^{r_4} \boldsymbol{E} \cdot d\boldsymbol{r} = \rho \int_{r_2}^{r_4} \boldsymbol{j} \cdot d\boldsymbol{r}$$

Whereas, when a field is present, the voltage difference becomes:

$$(V_4 - V_2)_B = \rho \int_{r_2}^{r_4} \boldsymbol{j}' \cdot d\boldsymbol{r} + \rho\mu_H \int_{r_2}^{r_4} (\boldsymbol{j}' \times \boldsymbol{B}) \cdot d\boldsymbol{r}$$

For point contacts, and assuming negligible magnetoresistivity, the current density field must remain invariant in the magnetic field (**j' = j**). The Hall voltage is then:

$$V_{H42} = (V_4 - V_2)_B - (V_4 - V_2)_0 = \rho\mu_H \int_{r_2}^{r_4} (j \times B) \cdot dr$$

The magnetic field is perpendicular to the sample (in the **x** direction), and the Hall voltage simplifies to $V_{H42} = \rho\mu_H BI/d$. The Hall coefficient is calculated from averaging V_{H42} and V_{H31}:

$$R_H = \frac{d}{B}\left[\frac{R_{31,24} + R_{42,13}}{2}\right] \quad (3)$$

where B is the magnetic field strength.

To minimize magnetoresistive and other effects, it is best to average over magnetic field polarities and current directions. The Hall coefficient for the sample becomes:

$$R_H = \frac{d}{B}\frac{1}{8}[R_{31,42}(+B) - R_{13,42}(+B) + R_{42,13}(+B) - R_{24,13}(+B) + R_{13,42}(-B) - R_{31,42}(-B) + R_{24,13}(-B) - R_{42,13}(-B)] \quad (4)$$

where +B and -B represent field polarities of the magnetic field.

The sign of the Hall coefficient reflects the majority of charge carriers in the material. If R_H is negative, the material is n-type, if R_H is positive, the material is p-type.

The next step in characterization of the p-type TCO is to calculate the mobility. There are different definitions of mobility, but here, we are concerned only with the Hall mobility and conductivity mobility. The two differ by a factor dependent on the scattering mechanisms, but here the approximation is that the two are equal. The conductivity (σ) of a semiconductor is

defined as: $\sigma = q(\mu_n n + \mu_p p)$, where q is charge in Coulombs, μ_n and μ_p are the mobilities of the electrons and holes, respectively, and n and p are the concentration of electrons and holes, respectively (Schroder, 1998). From the Lorentz force described above and in general for p-type semiconductors, the concentration p can be written in terms of the Hall coefficient as $p = 1/qR_H$ This was derived under simplifying conditions of energy-independent scattering. By including scattering, one obtains $p = r/qR_H$, where $r = \langle\tau^2\rangle/\langle\tau\rangle^2$ and τ is the mean time between carrier collisions (Schroder, 1998). The Hall mobility is:

$$\mu_H = \frac{|R_H|}{\rho} \tag{5}$$

with the relationship between Hall mobility and conductivity mobility

$$\mu_H = r\mu_p \tag{6}$$

But, as before, it is estimated that the scattering mechanisms are independent and thus $\mu_H = \mu_p$ (Schroder, 1998). Note that the magnitude of R_H is used and therefore does not have the information of carrier type with it in the calculation of μ_H. In general, p-type materials tend to have lower mobilities than n-type materials; often at least an order of magnitude lower. This is due in part to the higher effective mass of holes and that majority carriers experience ionized impurity scattering (Schroder, 1998).

For the Hall coefficient measurement, a magnetic field of 3200 G was used. The current

was generated by a Keithley 220 current source, and the voltage was measured with a Keithley 181 nano-voltmeter (sensitivity range 1 μV to 200 mV). The Keithley 181 nano-voltmeter appears to be stable to only 1 part in 1000. Therefore, since the Hall voltage is measured as a small difference of a larger background signal, the smallest measurable Hall voltage is 10^{-3} V_ρ or 1 μV (the limit of sensitivity), whichever is larger. Using equations (2), (4), (5) and that $I_{ij} = -I_{ji}$, it can easily be shown that the Hall mobility can be calculated as follows:

$$R_H = \frac{ln2}{B\pi} \frac{[(V_{42}^{B+} - V_{42}^{B-}) + (V_{13}^{B+} - V_{13}^{B-})]}{(V_{12} + V_{13} + V_{41} + V_{43})}$$

where the superscript B± represents the voltage measured in the corresponding direction of the magnetic field. Since the Hall mobility is proportional to $\Delta V_H/V_\rho$, where $\Delta V_H = V^{B+} - V^{B-}$ and V_ρ is the voltage measured for resistivity, the Hall mobility is limited by the voltages, V_ρ, generated during testing. For instance, if one measured 0.9 μV for V_ρ, V_ρ is really only stable to 1 μV and thus ΔV_H is only stable to 1 μV as well. Therefore, the Hall mobility has an upper bound of ln(2)/Bπ*(1 μV/1 μV). On the other hand, if one measures 200 mV for V_ρ, V_ρ is only stable to 0.2 mV, and therefore ΔV_H is also only stable to 0.2 mV. The Hall mobility thus has a lower bound of ln(2)/Bπ*(0.2 mV/200 mV) (see equations 2 and 4).The minimum and maximum Hall coefficients were determined to be 3.447 and 6894 cm^2/Vs, respectively. The calculations for these values are based on equations (2), (4), (5), and that the maximum difference calculable is only 1 part in 1000.

Theoretical plots of the Hall mobility versus resistivity were made (see Figs. 5 and 6) using

Matlab computational software. Figure 5 shows the basic area within which we would expect to measure Hall coefficients with limits placed by the instruments used. The curve on the right shows the lowest possible supply current (10 nA), and thus an upper bound of mobility. The curve at the lower left shows a lower cutoff if a current of 100 mA is used. The two solid lines at the top and bottom show the maximum and minimum values of measurable Hall mobilities, respectively. For reference, the measured data points of resistivity and mobility for two $CuAlO_2$ (circles) samples and ITO (x) are plotted as well. As can be seen, the ITO falls well within the range of measurable values while the $CuAlO_2$ samples are outside the range. Figure 6 is an estimate of how the Hall mobility is expected to vary with resistivity and a given measurement current. It has the same general characteristics of Figure 5, but shows curves for values of current ranging from 10 nA to 100 mA. The curves define a lower bound that can be measured for the mobility of a sample. For example, a sample has a resistivity of 1×10^{-2} Ωcm and various currents ranging from 10 μA to 0.1 μA are used to measure the mobility. If the data from the tests using currents between 10 μA to 1 μA all return valid mobility values, but the tests using currents below 1 μA result in artificial mobility values, then the minimum current resulting in valid mobility measurements of this example is 1 μA. Thus since this example has a resistivity of 1×10^{-2} Ωcm and a minimum supply current of 1 μA, only mobilities ranging from 3.447 and ~ 80 cm^2/Vs can be considered valid measurements.

Samples of GaAs and ITO were used to calibrate the system. Multiple room temperature measurements of these two samples yielded average values for resistivity and mobility of 5.473×10^{-2} Ωcm and 4364.3 cm^2/Vs for GaAs, and 1.061×10^{-4} Ωcm and 33.3 cm^2/Vs for ITO,

respectively (see Table 1 for measured values). The thickness of the GaAs sample was not known but was assumed to be 1 μm for all measurements. Thus, the resistivity is only known to within a factor of the real thickness (*d*/1 μm). There are no independent measurements available for the GaAs and ITO samples, but these are close to expected and accepted values (typical values for ITO are around 10^{-4} Ωcm and 24 cm^2/Vs). A low-temperature test of ITO was made at 77 K to compare it to room temperature (RT, 300K) data. At RT, this test yielded a mobility of 28.8 cm^2/Vs and resistivity of 1.296 x 10^{-4} Ωcm. At 77K, the mobility increased to 32.8 cm^2/Vs, and the resistivity remained fairly stable at 1.138 x 10^{-4} Ωcm. This may be a spurious data point since the low-temp test did not return a higher mobility than the average of the previous RT tests. It is unknown what the cause of error might be. Typical semiconductors experience an increase their mobility when at lower temperatures, which we should expect to see for ITO as well (Look, 1998). The system errors should be small and any errors in measurements should be primarily due to contact size as discussed earlier. Of course, this is only true for materials which have a measurable Hall effect, otherwise the Hall measurements are inconclusive.

To corroborate the Hall coefficient measurements for carrier type, hot-probe measurements were conducted to qualitatively determine the majority carrier type. The instrument used was a Leeds and Northrup hot-probe galvanometer. A thermal current is generated in the sample by application of a hot probe, usually a few degrees above room temperature, on the surface. A cold probe is also in contact with the sample, but away from the hot probe so that it remains at a different temperature. As the current passes through the circuit (see, Fig. 5) the galvanometer deflects in opposite directions corresponding to n or p-type

conduction. Theoretically, this system can be used with the knowledge of the temperature gradient for calculations of the Seebeck coefficient with the following formula:

$$S = \frac{\Delta V}{\Delta T} \quad (\mu V/K)$$

here, for the present experimental system (see Fig. 3),

$$\Delta V = (0.025 \ \mu A/mm)(X_{mm})([R_s^{-1} + (R_{pot} - R_2)^{-1}]^{-1} + R_2 + R_G)$$

X_{mm} is the galvanometer deflection in mm, R_s is the sample resistance, R_{pot} is the potentiometer resistance (700 Ω), 0.025 μA/mm is the sensitivity of the galvanometer, ΔT is the measured temperature gradient from hot probe to cold probe, and R_G is the resistance of the galvanometer. Unfortunately, the inability to measure ΔT and the instability of the instrument prevented reproducible and quantitative values for calculation of the Seebeck coefficient.

Three different compositions of materials, $YCaCuO_2$, $YCaSnCuO_2$, and $CuAlO_2$ were tested for resistivity and Hall mobility (see Table 2 for measured values). Measurements on all samples were conducted over several days and using different sample orientations to prevent any possible equipment errors from affecting the data. As can be seen, except for samples #49 and #50, the resistivities measured are within acceptable values. This is determined from the coefficient of variance (C.O.V.). The C.O.V, defined as the standard deviation divided by the mean, times 100, has an upper limit of 10% for which values above are considered uncorrelated while those below are considered valid and within experimental errors (Hawkins and Weber, 1980). For most of the samples, the C.O.V. of resistivity is well below 10%. On the other hand,

the C.O.V.s for the Hall coefficient and mobility are much worse. This would indicate that the materials under test do not have a measurable Hall effect.

Another important factor which determines whether the Hall mobility is accurate is if the Hall voltages with an applied magnetic field are symmetric about the Hall voltage without an applied field. That is, the voltages measured with an applied field should be smaller or larger than the voltages measured without an applied field. If they are not symmetric, errors occur in the calculation of the Hall mobility and incorrect values are reported. Both of the calibration samples exhibited values for the Hall voltages which were symmetric with respect to the Hall voltage without a magnetic field. Unfortunately, the materials under test did not exhibit symmetrical Hall voltages. Although the materials did exhibit measurable resistivities that are within experimental errors, they did not have a measurable Hall effect. For future work, a more accurate and stable voltmeter would increase the sensitivity and allow for smaller mobilities to be measured.

Table 1: Calibration Sample Data (B=3200G)

Sample	Current (mA)	Thickness (um)	Resistivity (Ohm.cm)	Hall Coefficient (cm^3/C)	Mobility (cm^2/Vs)
GaAs					
Test #1	0.1	1	5.424E-02	-2.400E+02	4432.6
Test #2	0.5	1	5.401E-02	-2.390E+02	4427.1
Test #3	0.1	1	5.510E-02	-2.370E+02	4302.4
Test #4	0.5	1	5.463E-02	-2.370E+02	4335
Test #5	0.5	1	5.510E-02	-2.370E+02	4302.4
Test #6	0.5	1	5.463E-02	-2.370E+02	4335
Test #7	0.5	1	5.502E-02	-2.410E+02	4382.9
Test #8	0.5	1	5.508E-02	-2.420E+02	4396.8
Average			5.473E-02	-2.388E+02	4364.275
Stnd. Dev			3.967E-04	-1.920E+00	49.233
% C.O.V.			0.725	0.804	1.128
ITO					
Test #1	30	0.25	1.061E-04	-3.560E-03	33.5
Test #2	30	0.25	1.061E-04	-3.460E-03	33.5
Test #3	40	0.25	1.061E-04	-3.500E-03	33
Test #4	1	0.25	1.060E-04	-3.520E-03	33.2
Average			1.061E-04	-3.510E-03	33.3
Stnd. Dev			2.958E-08	-3.606E-05	0.212
% C.O.V.			0.028	1.027	0.637
Low T test					
300 K	5	0.25	1.296E-04	3.73E-03	28.8
77 K	5	0.25	1.138E-04	3.73E-03	32.8

Table 2: Test Sample Data (B=3200G)

Sample	Current (mA)	Thickness (um)	Resistivity (Ohm.cm)	Hall Coefficient (cm^3/C)	Mobility (cm^2/Vs)
YCaCuO2 #49					
Test #1	0.0001	0.2	6.739E+00	-1.150E+02	17
Test #2	0.001	0.2	6.823E+00	-2.420E+01	3.5
Test #3	0.0001	0.2	9.209E+00	-7.810E+00	0.8
Average			7.590E+00	-4.900E+01	7.1
Stnd. Dev			1.145E+00	-4.714E+01	7.087
% C.O.V.			15.086	96.206	99.811
YCaCuO2 #50					
Test #1	0.001	0.1	5.704E+00	1.360E+01	2.4
Test #2	0.0001	0.1	5.505E+00	4.885E+01	8.9
Test #3	0.0001	0.1	3.790E+00	2.440E+00	0.6
Average			5.000E+00	2.163E+01	3.967
Stnd. Dev			8.592E-01	1.978E+01	3.565
% C.O.V.			17.185	91.444	89.873
YCaCuO2 #51					
Test #1	0.0005	0.2	8.662E+00	-8.220E+01	9.5
Test #2	0.0001	0.2	8.887E+00	1.170E+01	1.3
Test #3	0.0001	0.2	8.720E+00	-1.360E+02	15.6
Average			8.756E+00	-6.883E+01	8.800
Stnd. Dev			9.538E-02	6.103E+01	5.859
% C.O.V.			1.089	-88.670	66.578
YCaCuO2 #53					
Test #1	0.0001	0.2	4.668E+01	-1.160E+02	2.5
Test #2	0.0001	0.2	5.108E+01	5.940E+02	11.6
Average			4.888E+01	2.390E+02	7.050
Stnd. Dev			2.200E+00	3.550E+02	4.550
% C.O.V.			4.501	148.536	64.539

Table 2: Test Sample Data (B=3200G)

Sample	Current (mA)	Thickness (um)	Resistvity (Ohm.cm)	Hall Coefficient (cm^3/C)	Mobility (cm^2/Vs)
YCaSnCuO2 #73					
Test #1	10	0.4	6.715E-04	-5.000E-04	0.7
Test #2	0.1	0.4	6.609E-04	-1.560E-03	2.4
Test #3	1	0.4	6.608E-04	-6.250E-04	0.9
Test #4	10	0.4	6.608E-04	7.810E-05	0.1
Test #5	14	0.4	6.609E-04	7.810E-05	0.1
Average			6.630E-04	-5.058E-04	0.840
Stnd. Dev			4.268E-06	6.012E-04	0.843
% C.O.V.			0.644	-118.879	100.340
YCaSnCuO2 #93					
Test #1	0.001	0.4	8.220E-04	1.560E-01	190.1
Test #2	0.01	0.4	9.503E-04	1.560E-02	16.4
Test #3	1	0.4	9.609E-04	1.560E-04	0.2
Test #4	2	0.4	9.609E-04	1.560E-04	0.2
Test #5	5	0.4	8.739E-04	1.880E-04	0.2
Average			9.136E-04	3.442E-02	41.420
Stnd. Dev			5.619E-05	6.108E-02	74.604
% C.O.V.			6.151	177.464	180.117
CuAlO2 #002					
Test #1	0.0005	0.15	1.611E+01	-2.090E+01	1.3
Test #2	0.0005	0.15	1.639E+01	2.120E+02	13
Test #3	0.0005	0.15	1.642E+01	-5.740E+01	3.5
Average			1.631E+01	4.457E+01	5.933
Stnd. Dev			1.396E-01	1.193E+02	5.077
% C.O.V.			0.856	267.750	85.567

Table 2: Test Sample Data (B=3200G)

Sample	Current (mA)	Thickness (um)	Resistvity (Ohm.cm)	Hall Coefficient (cm^3/C)	Mobility (cm^2/Vs)
CuAlO2 #003					
Test #1	0.0005	0.1	7.658E+00	-2.130E+01	2.8
Test #2	0.0005	0.1	7.971E+00	1.720E+00	0.2
Average			7.815E+00	-9.790E+00	1.500
Stnd. Dev			1.565E-01	1.151E+01	1.300
% C.O.V.			2.003	-117.569	86.667
CuAlO2 #008					
Test #1	0.0002	0.23	4.393E+01	2.710E+02	6.2
Test #2	0.0002	0.23	4.477E+01	6.290E+00	0.1
Average			4.435E+01	1.386E+02	3.150
Stnd. Dev			4.200E-01	1.324E+02	3.050
% C.O.V.			0.947	95.463	96.825

Figure 1: van der Pauw Test Setup

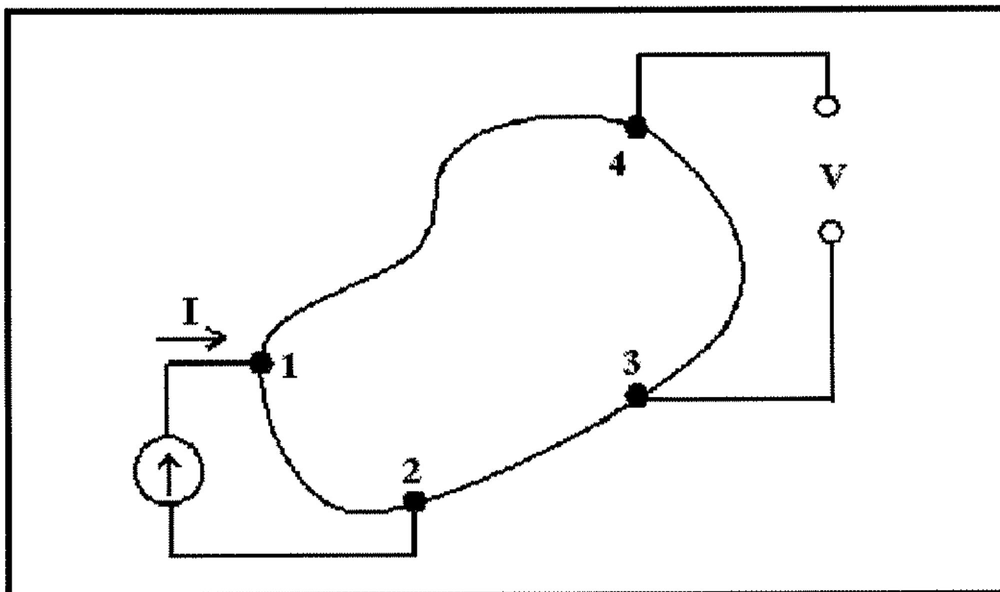

1a) van der Pauw Resistivity test setup

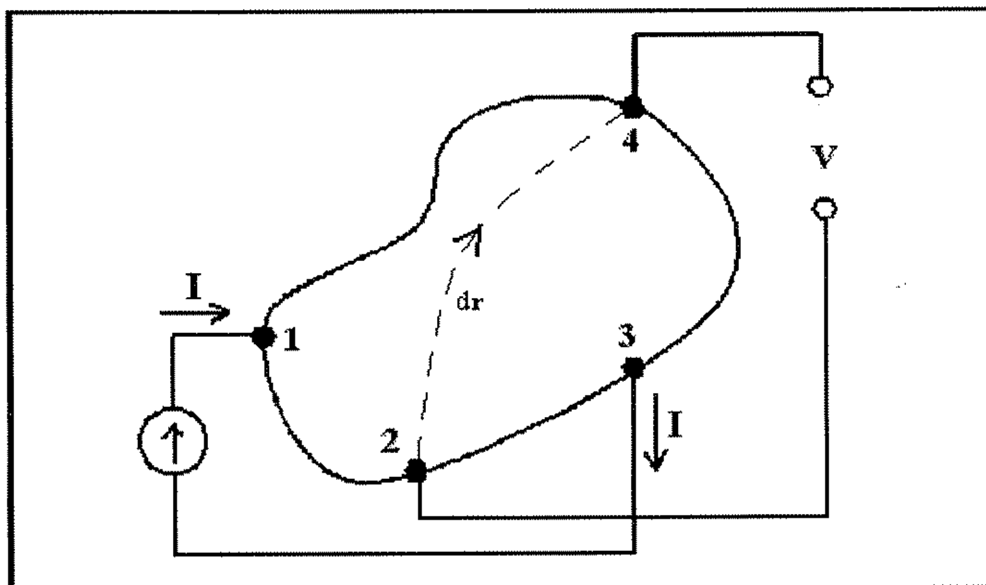

1b) van der Pauw Hall Coefficient test setup

Figure 2: Hall Bar in Magnetic Field

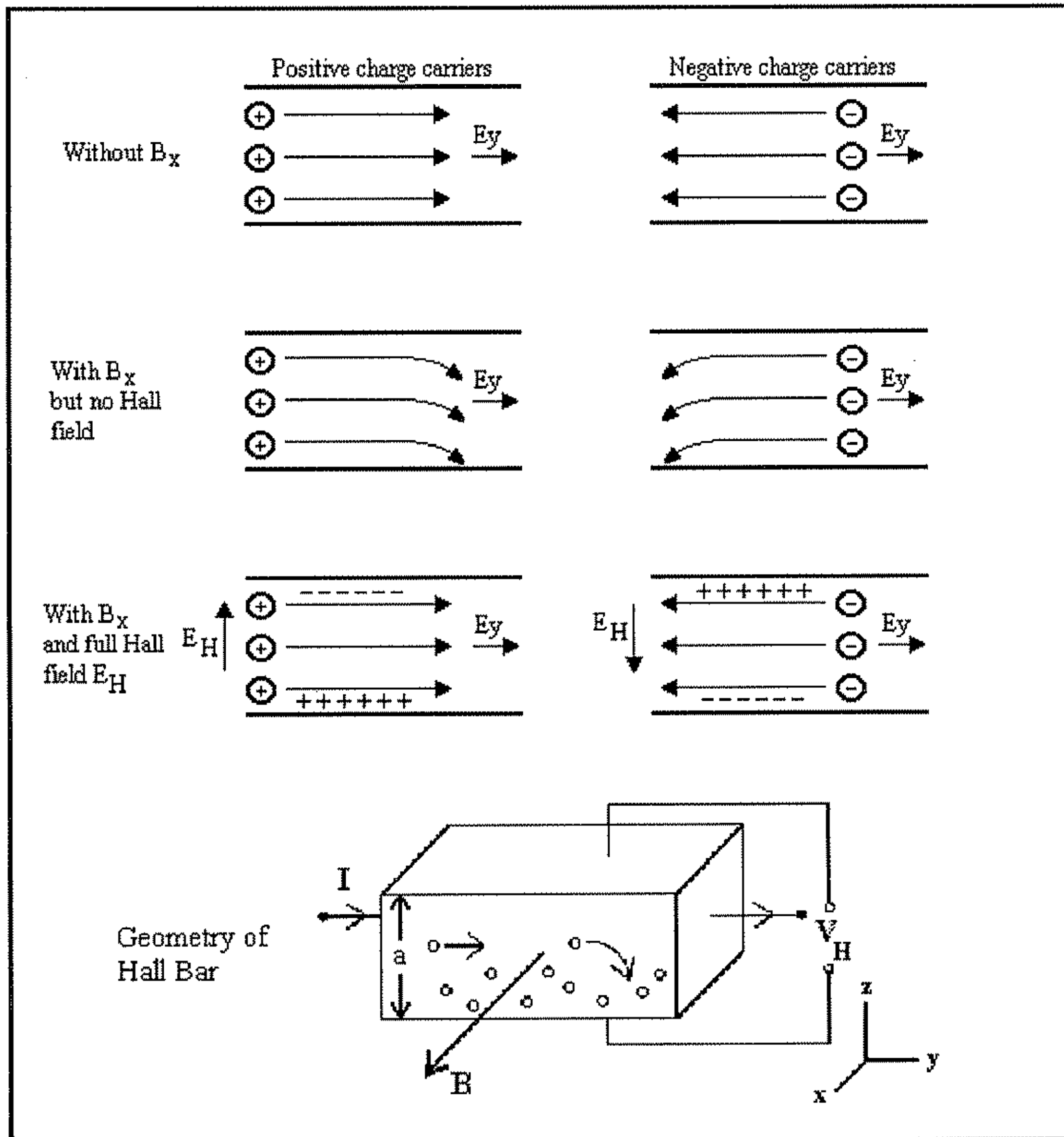

Figure 3: Effective Hot Probe Circuit

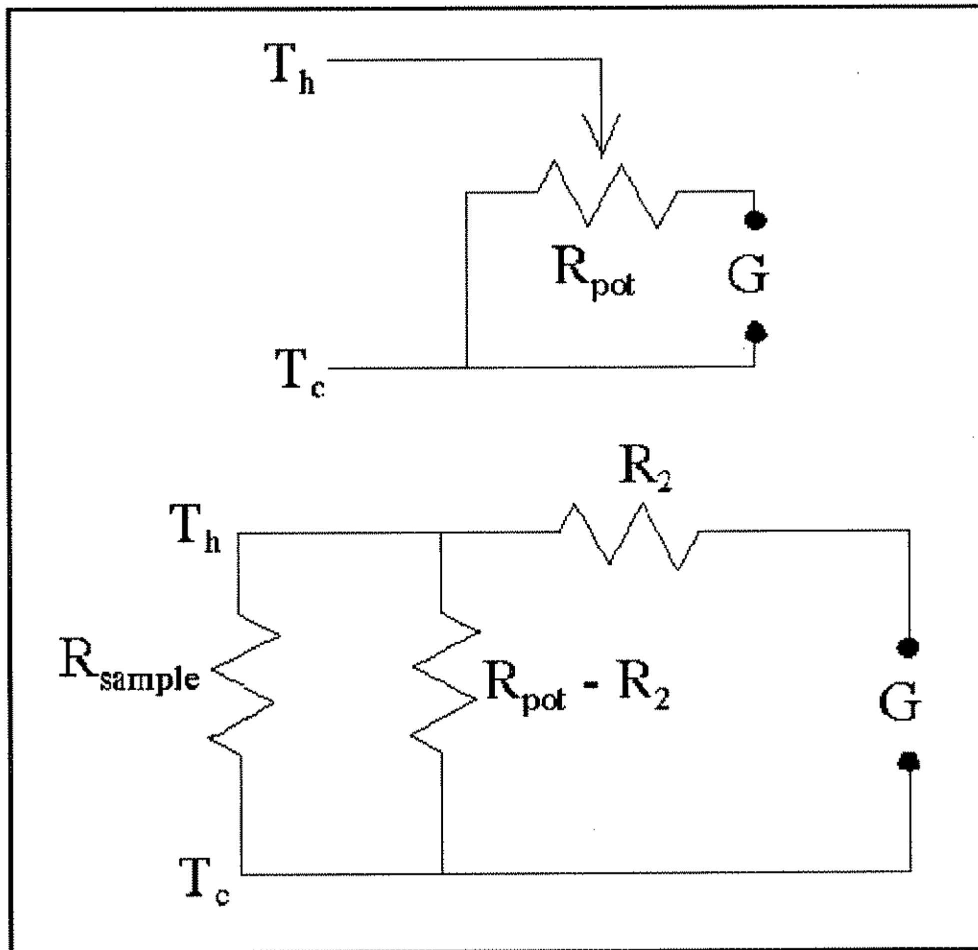

Figure 4: Contact Error Corrections

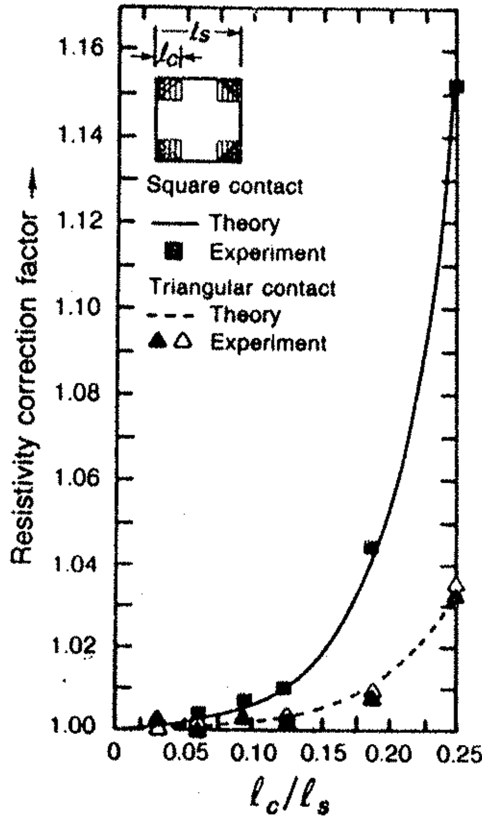

Fig. 1.1.10 Contact-size correction factors for the resistivity of a square pattern. (After Chwang *et al* (1974). Reproduced by permission of Pergamon Press)

4a) Resistivity correction due to contact erorrs.

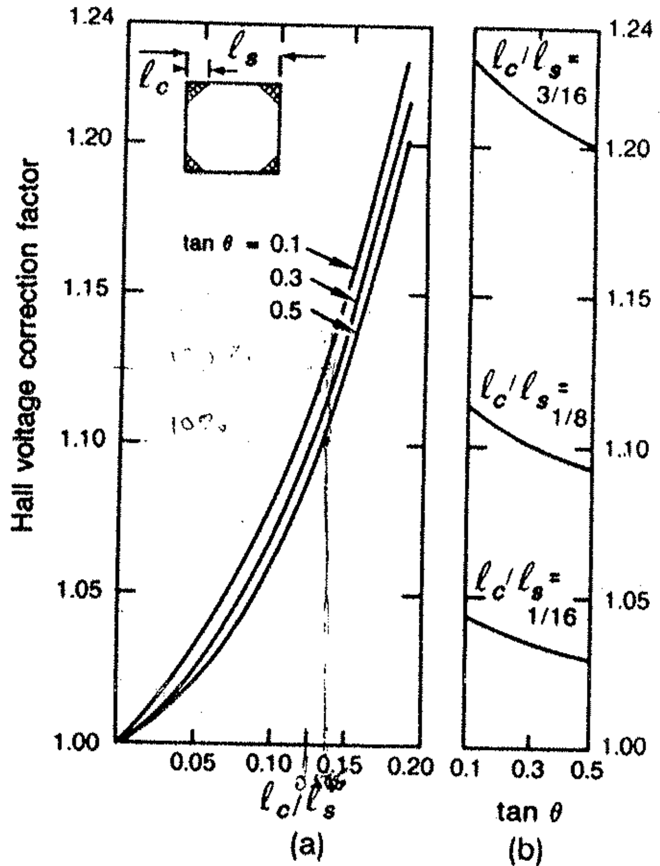

Fig. 1.1.11 Contact-size correction factors for the Hall voltage of a square pattern. Here θ is the Hall angle, defined as $\tan\theta = -E_y/E_x \simeq -\mu B$. (After Chwang *et al.* (1974). Reproduced by permission of Pergamon Press)

4b) Hall Coefficient correction due to contact errors

Graphs are taken from Look

Figure 5: Hall Mobility Limitation due to Instruments

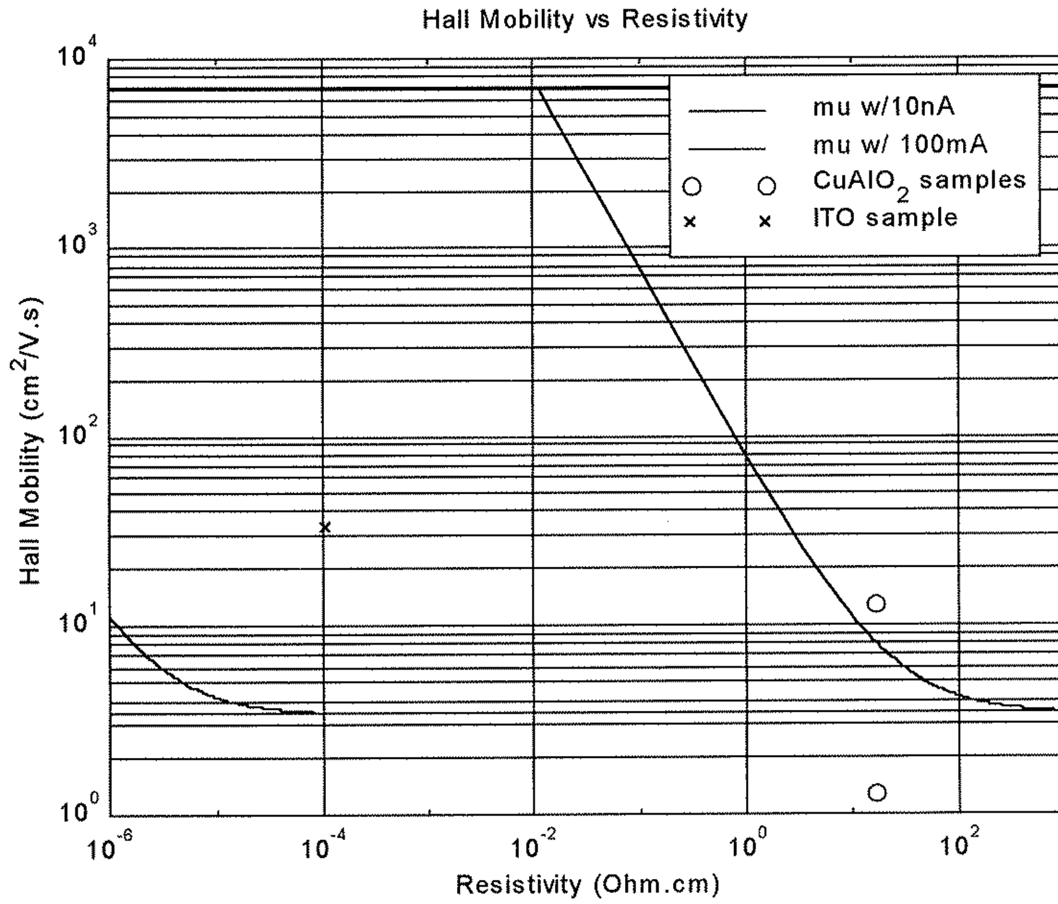

Figure 6: Hall Mobility versus Resistivity for Various Values of Current

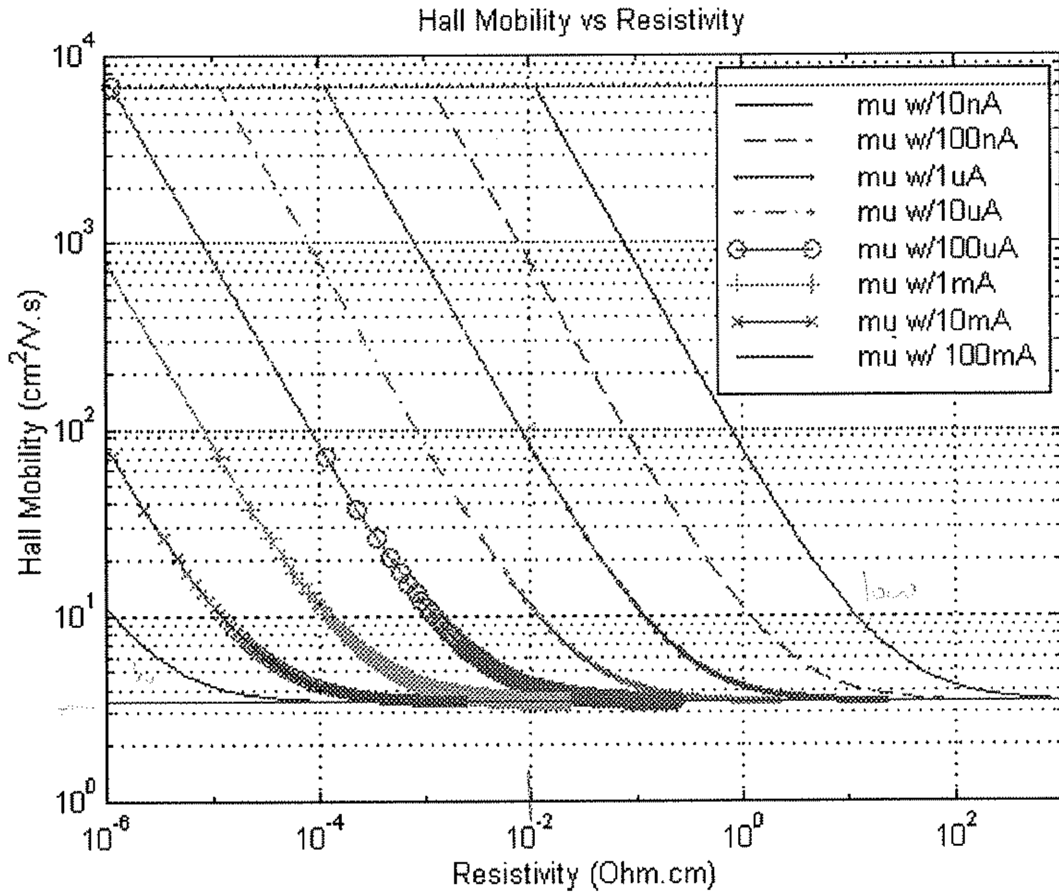

References:

Benko, F. A., Koffyberg, F. P., "The Optical Bandgap and Band-edge Positions of Semiconducting *p*-type $CuYO_2$," *Can. J. Phys.*, 63, 1985, pp. 1306-1308.

DeMey, G., "Potential Calculations in Hall Plates," *Advances in Electronics and Electron Physics*, vol. 61, (Eds, L. Marton and C. Marton), 1983, pp. 1-61, Academic, New York.

Hawkins, C. A., Weber, J. E., Statistical Analysis Applications to Business and Economics, Harper and Row, 1980, p. 34-35.

Putley, E.H., The Hall Effect and Related Phenomena, Butterworths, 1960, pp. 27, 42-46.

Hurd, C. M., The Hall Effect in Metals and Alloys, Plenum, 1972, pp. 5-7, 119, 276-286.

Kawazoe, H., Yasukawa, M., Hyodo, H., Kurita M., Yanagi, H., Hosono, H., "P-type electrical conduction in transparent thin films of $CuAlO_2$," *Nature*, vol. 389, 1997, pp. 939-942.

Kudo, A., Yanagi, H., Hosono, H., Kawazoe, H., "$SrCu_2O_2$: A p-type conductive oxide with wide band gap," *Applied Physics Letters*, vol. 73, pp. 220-222.

Lide,D. L., CRC Handbook of Chemistry and Physics 80th ed., CRC Press, 1999, p. 12-45.

Look, D., Electronic Characteristics of GaAs Materials and Devices, John Wiley and Sons, 1989, pp 1-21.

Morgan, J. H., Brodie, D. E., "The Preparation and Some Properties of Transparent Conducting ZnO for Use in Solar Cells," *Can. J. Phys.*, 60, 1982, pp. 1387-1390.

Otabe, T., Ueda, K., Kudoh, A., Hosono, H., Kawazoe, H., "N-type electrical conduction in transparent thin films of delafossite-type $AgInO_2$," *App. Phys. Letters*, vol. 72, 1998, pp. 1036-1038.

References (cont'd):

Schroder, D., Semiconductor Material and Device Characterization, John Wiley and Sons, 1998, pp. 509-517.

Thomas, G., "Invisible Circuits," *Nature*, vol. 389, Oct. 1997, pp. 907-908.

Wells, A. F., Structural Inorganic Chemistry 5th ed., Clarendon Press, 1984, pp. 271-271, 577-578.